The Astronomical Journal, 124:2920–2930, 2002 November

DETECTION OF ^{12}CO $J = 1 \rightarrow 0$ AND $J = 2 \rightarrow 1$ EMISSION FROM THE LUMINOUS BLUE VARIABLE AG CARINAE: CIRCUMSTELLAR ENVELOPE OR DISK?[1]

A. Nota,[2,3] A. Pasquali,[4] A. P. Marston,[5] H. J. G. L. M. Lamers,[6] M. Clampin[2] and R. E. Schulte-Ladbeck[7]

Received 2000 September 8; accepted 2002 July 25

ABSTRACT

We present the first detection of ^{12}CO $J = 2 \rightarrow 1$ and $J = 1 \rightarrow 0$ emission from the luminous blue variable AG Carinae. We show that AG Car resides in a region that is very rich in molecular gas with complex motions. We find evidence of a slow outflow of molecular gas, expanding at $\simeq$7 km s^{-1}. This emission appears spatially unresolved. We argue that it is spatially localized, rather than extended, and possibly associated with the immediate circumstellar region of AG Car. Both detected CO lines are characterized by a pseudo-Gaussian profile with FWHM $\simeq$ 15 km s^{-1}, indicating a slowly expanding region of molecular gas in close proximity to the hot central star. We have explored two possible scenarios to explain the observed profile: a circumstellar envelope, similar to carbon stars, or a circumstellar disk. The option of the circumstellar disk is preferable because (1) it is consistent with additional independent indications of the existence of wind asymmetries in close proximity to the central star, found from spectropolarimetry and analysis of the UV and optical line profiles, and (2) it provides the conditions of density and shielding necessary for the survival of the CO molecules in proximity to such a hot star ($T_{\rm eff} \simeq$ 14,000–20,000 K). On the assumption that the CO emission originated when AG Car was in an evolved state, we derive a lower limit to the CO mass of $6.5 \times 10^{-3}\ M_{\odot}$. We also estimate that the CO fraction is $\simeq 2.3 \times 10^{-3}$ of the total mass of molecular gas, which then would amount to 2.8 $M_{\odot}$. This is smaller, but still comparable to, the mass of ionized gas present in the circumstellar environment (4.2 $M_{\odot}$), with the implication that the molecular gas fraction can contribute significantly to the overall mass lost from the central star in its post–main-sequence evolution.

Key words: circumstellar matter — stars: individual (AG Carinae) — stars: variables: other

1. INTRODUCTION

Massive stars spend their hydrogen-burning phase as O stars and become, after a few million years, Wolf-Rayet (W-R) stars undergoing core helium burning. Mass loss plays a key role in driving the stellar evolution from the main sequence to the W-R stage, especially during the intermediate luminous blue variable (LBV) phase. LBVs have been recognized to be at the point of exhausting their core hydrogen burning (Pasquali et al. 1997). In the Hertzsprung-Russell (H-R) diagram they are located close to the Humphreys-Davidson boundary (Humphreys & Davidson 1979), which represents an empirical instability limit to the evolution of stars more massive than 40 $M_{\odot}$. They display large and irregular spectrophotometric variability, passing between phases of hot visual minima ($T_{\rm eff} \sim$ 20,000–30,000K) and phases of cooler visual maxima ($T_{\rm eff} <$ 10,000K). Their variability is also characterized by violent eruptions, with visual brightness increases of 3 mag or more, and extreme mass loss (up to several solar masses of material ejected into the surrounding medium). Between such dramatic outbursts, LBVs still lose mass at high rates—typically 10^{-5}–$10^{-4}\ M_{\odot}\ {\rm yr}^{-1}$ (see, e.g., Leitherer et al. 1994).

The relics of these eruptions are spectacular circumstellar nebulae, such as that observed around η Carinae. A systematic investigation of LBVs in the Galaxy and in the Large Magellanic Cloud (Nota et al. 1995) has shown that the majority of the known LBVs are surrounded by an ejected nebula, whose kinematic and chemical properties may be used to constrain the mass-loss history of the central star. The morphology of these nebulae suggests that they are shaped by wind interactions. The nebular dynamics indicates that the ejection timescale is comparable to the evolutionary lifetime of the LBV phase. Their chemical composition has been used to infer the evolutionary status of the central star at the moment of the ejection (Lamers et al. 2001). However, these evolutionary diagnostics are mostly derived from optical data. So far, LBVs have been little studied at infrared or submillimeter wavelengths, although these spectral regions provide a number of diagnostic probes of the nebular physical conditions that are not available at optical or UV wavelengths. A great wealth of information can be derived from such observations regarding the presence of dust or molecular gas in the close surroundings of these hot stars, to complement the optical data and to help determine the total amount of mass lost during the LBV phase. This piece of information, presently incomplete, is crucial to constraining the theoretical models, which currently fail to reproduce the transition between O and W-R stars (Langer et al. 1994).

[1] Based on observations collected at the European Southern Observatory, La Silla, Chile.

[2] Space Telescope Science Institute, 3700 San Martin Drive, Baltimore, MD 21218; nota@stsci.edu, clampin@stsci.edu.

[3] On assignment from the Space Telescope Operations Division of the European Space Agency.

[4] Space Telescope European Coordinating Facility, Karl-Schwarzschild-Strasse 2, D-85748 Garching, Germany; apasqual@eso.org.

[5] *SIRTF* Science Center, Mail Code 314-6, California Institute of Technology, 1200 East California Boulevard, Pasadena, CA 91125; tmarston@ipac.caltech.edu.

[6] Sterrekundig Instituut, Universiteit Utrecht, Postbus 80000, NL-3508 TA Utrecht, Netherlands; and SRON Laboratory for Space Research; lamers@astro.uu.nl.

[7] Department of Physics and Astronomy, University of Pittsburgh, 3941 O'Hara Street, Pittsburgh, PA 15260; rsl@phyast.pitt.edu.

In the past few years, near-infrared imaging and spectroscopy, both from the ground and, more recently, with the *Infrared Space Observatory* (*ISO*) (Waters et al. 1998, 1999; Voors et al. 1997; Morris et al. 1999), have greatly expanded our understanding of the properties and formation and survival mechanisms of dust in hot stellar environments ($T_{\rm eff} \simeq$ 20,000–40,000 K). For the first time it has been possible to study the spatial distribution of the dust, to quantify the nebular dust mass with some accuracy, and to investigate the dust-gas correlation. In addition, spectroscopic investigation of the dust's features has contributed to a better characterization of the dust properties and has provided additional independent evidence that these stars were cool and extended (mimicking a red supergiant) during the ejection of the nebula (Lamers et al. 2001).

The presence of molecular gas around hot, evolved stars was unexpectedly detected by McGregor, Hillier, & Hyland (1988) in a survey of blue supergiants in the Large Magellanic Cloud. They unambiguously detected the first-overtone band heads of CO at 2.3 μm in six objects. Given the very low CO dissociation energy (11.1 eV), the presence of CO emission in close proximity to O and B supergiants, characterized by fast stellar winds ($V_{\rm inf} \simeq$ 200–400 km s^{-1}) and strong radiation fields, has been difficult to explain. One possible explanation is that the CO emission is spatially extended and far from the star. If the star has already experienced a red supergiant (RSG) phase, the CO emission could be a tracer of the previous cool and dense wind, which has been compressed and excited by the interaction with the present, hotter stellar wind. Alternatively, the CO emission may be localized and close to the star. McGregor et al. (1988) tentatively identified the emitting CO region with a circumstellar disk that is able to shield the CO from the stellar radiation and ionized wind. Localized emission can also be explained, as is observed in the case of cooler giants and supergiants (such as S and C stars), by the survival of the CO in an outer layer of the stellar envelope and its excitation by the stellar radiation field (Knapp & Morris 1985; Olofsson, Eriksson, & Gustafsson 1988; Heske 1990). This explanation is only acceptable if the star mimicked an RSG during the ejection of the nebula. Unfortunately, the observations by McGregor et al. did not have the spatial resolution necessary to discriminate among the possible scenarios.

Among the luminous supergiants that McGregor et al. (1988) observed was the Galactic LBV AG Carinae. AG Car is one of the most luminous LBVs, being located in the H-R diagram very close to the Humphreys-Davidson limit. Its distance is 6 ± 1 kpc and its luminosity is $1.7 \times 10^6\ L_\odot$ (Humphreys et al. 1989). The effective temperature is variable between about 9000 and 25,000 K, and so the radius changes from 70 to 500 $R_\odot$ (Lamers 1986; Voors et al. 2000). It is surrounded by a very bright, extended nebula that has been known since the 1950s (Thackeray 1950). The nebula is composed of ionized gas and dust. When imaged in the light of Hα, it exhibits an elliptical shell-like morphology ($30'' \times 40''$ in size). The nebular lines indicate that the nebula is expanding at an average velocity of 70 km s^{-1} (Smith 1991). In the light of the line-free continuum, which displays the stellar radiation scattered by dust, the AG Car nebula appears quite different (Paresce & Nota 1989): the dust grains are distributed in a jetlike feature, which the *Hubble Space Telescope* has resolved into a myriad of clumps and filaments with an overall bipolar structure (Nota et al. 1996). Recent *ISO* observations indicate that the dust grains are mostly crystalline olivine, with an emission peak at 33.8 μm (Waters et al. 1999). McGregor et al. (1988) did not detect any CO overtone emission in AG Car. They found little or no emission from hot dust in the near-infrared but, surprisingly, detected strong far-infrared emission from cool dust, and they inferred the action of a strong stellar wind, which possibly removed the dust from the inner region. We decided to revisit the question of the presence of molecular gas in the circumstellar environment of AG Car, for a number of reasons: AG Car is the ideal target for a neutral-material study, given its proximity and the large spatial extension of the nebula. The nebula is rich in gas and dust and displays a strong far-infrared excess. We have therefore decided to start an investigation aimed at detecting and characterizing the properties of the neutral material around AG Car, with the objective to (1) detect CO emission from molecular gas, (2) understand whether the emission is localized or spatially extended, and (3) determine the amount of molecular gas in the circumstellar environment. We have carried out this program with the Swedish-ESO Submillimetre Telescope (SEST), studying the transitions ^{12}CO $J = 2 \rightarrow 1$ and $J = 1 \rightarrow 0$ and obtaining CO emission maps of the entire nebula. The observation strategy and data reduction procedures are described in § 2, and the results of our investigation are presented in § 3. Discussion and conclusions follow in §§ 4 and 5, respectively.

2. OBSERVATIONS AND DATA REDUCTION

Observations of the region around AG Car were made with SEST in 1997 February, 1998 March, and 1999 February. In 1997 February, observations were made with the 3 mm receiver and high-resolution spectrometer (HRS) covering the ^{12}CO $J = 1 \rightarrow 0$ (115.271 GHz) emission line. This provided 2000 frequency channels covering an 86 MHz bandwidth. The frequency resolution of this system is 80 kHz, providing a velocity resolution of approximately 0.22 km s^{-1}. At this wavelength, SEST has a beamwidth of approximately 45″. Single-beam spectra were taken along an east-west strip from 12′ east of AG Car to 15′ west of AG Car using 45″ steps. A total of 36 spectra were acquired, with typical on-source integration times of 30 s. A dual beam-switching method was used in which the source was alternately placed in the two beams to eliminate baseline ripples. The beam throw was 11.′6. For several of the positions, emission in the off-source beams affected our final profile. The corresponding spectra were therefore discarded during our analysis.

Additional observations were taken with the same configuration on 1999 February 28, with the objective of extending the spatial coverage to 30′ to the east and to the west of AG Car. Typical exposure times were 30 s to 2 minutes. A smaller mapping in declination was performed in the same configuration, from 0′ to 10′ north and south, with pointings at 0′, −2′, −10′, +2′, and +10′. In Figure 1, we show a large-field image centered on AG Car, generated from Palomar Observatory Sky Survey plates, on which we have drawn the region covered by the ^{12}CO $J = 1 \rightarrow 0$ observations.

Observations were made of the southwest quadrant of AG Car nebula in 1998 March, using the 230 GHz receiver with HRS centered on the ^{12}CO $J = 2 \rightarrow 1$ (230.537 GHz) emission line. We concentrated on this spatial region first, because optical images show the highest concentration of gas emitting and dust scattering stellar light. The complete

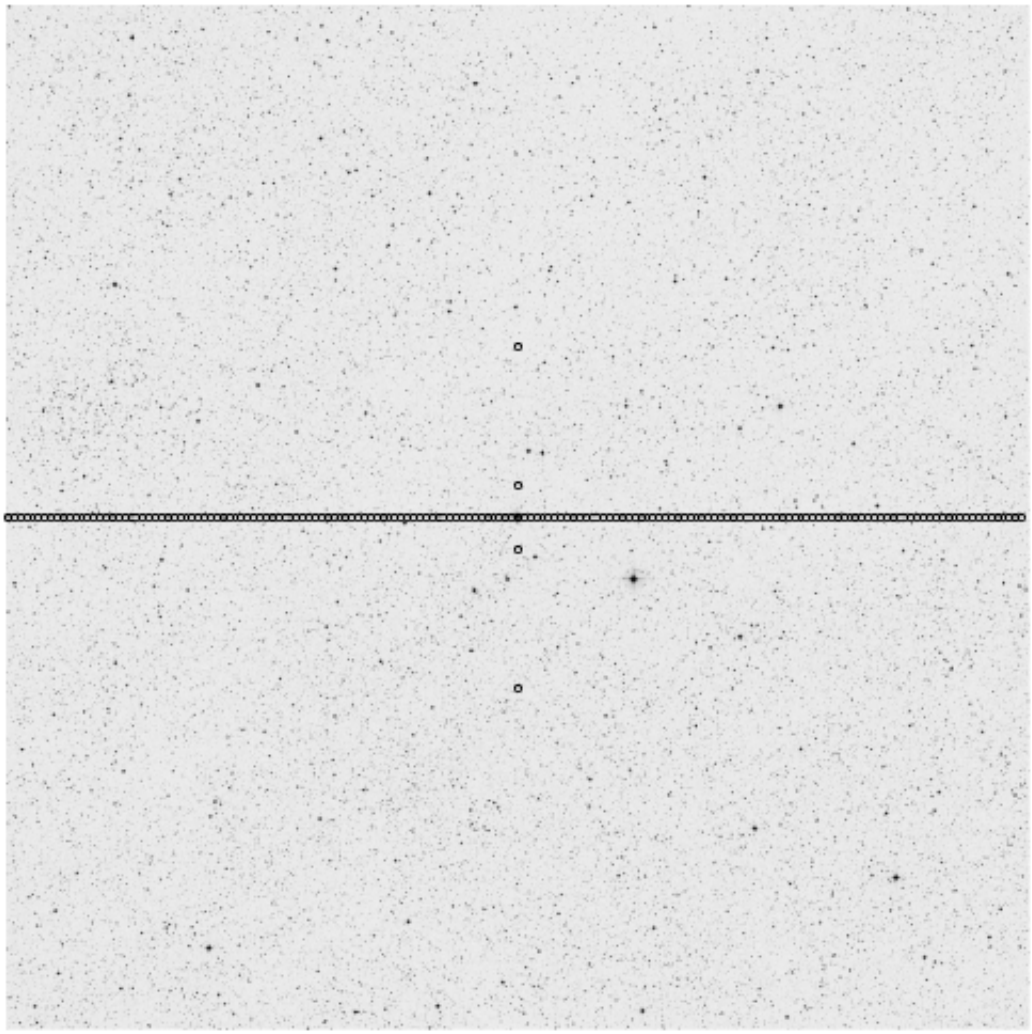

FIG. 1.—A 30′ × 30′ optical image of the region around AG Car (center) showing the position of the ^{12}CO $J = 1 \rightarrow 0$ observations. The size of the symbols is matched to the size of the beam. North is up and east is to the left.

mapping of the nebula was achieved in 1999 February, with the other three quadrants covered. At these frequencies, our velocity resolution is 0.11 km s^{-1} and the effective beamwidth of the telescope is 23″. The observations of the southwest quadrant covered a regular grid of 36″ × 36″ at 12″ intervals, starting at the position of the star. The southeast quadrant covered a grid of nine observations, to 24″ south, also spaced by 12″. The northeast quadrant covered nine pointings extending to 36″ east, symmetric to the southwest quadrant, and finally the northwest quadrant covered nine pointings, also spaced by 12″. In Figure 2, we show all pointings overlaid on a ground-based coronagraphic image of the AG Car nebula, taken in the light of Hα (Nota et al. 1992). Several on-source observations were made at each grid position, with 30 s integration each. Summation of these spectra provided total on-source integration times of 5–10 minutes at each of the grid positions. Elimination of baseline ripples was achieved by position switching to an area of the sky apparently devoid of CO emission lines.

For both sets of observations, pointing to better than 3″ was achieved through observations of bright SiO masers, for example, VY CMa. Intensity calibration, resulting in an antenna temperature T_A^*, was provided by the chopper-wheel method and a set of internal calibrators. This was done on-line as the data were collected at the telescope. Linear drifts in frequency were also removed during each calibration through the use of a frequency comb (a set of narrow lines with well-defined frequencies). To convert the intensities to main-beam brightness temperatures ($T_{\rm mb}^*$), the antenna temperatures were divided by the main-beam efficiency of the telescope (0.7 and 0.5 at 115 and 230 GHz, respectively). For both sets of observations, constant and/or residual sinusoidal baselines were removed, as necessary, from each of the final CO profiles. The resulting profiles were then plotted on a velocity scale after being reduced to the local standard of rest ($V_{\rm lsr}$).

3. CO MAPS AND CO LINE PROFILES

The ^{12}CO $J = 2 \rightarrow 1$ and $J = 1 \rightarrow 0$ profiles taken at the star's position are plotted in Figure 3. They are both characterized by a broad component, with a FWHM of $\simeq$15 km s^{-1} centered on the star, and by two narrow components, which in the ^{12}CO $J = 1 \rightarrow 0$ profile have FWHMs of 2 and 1.2 km s^{-1}, respectively, and are separated in velocity by approximately 10 km s^{-1}. The first goal of this work is to

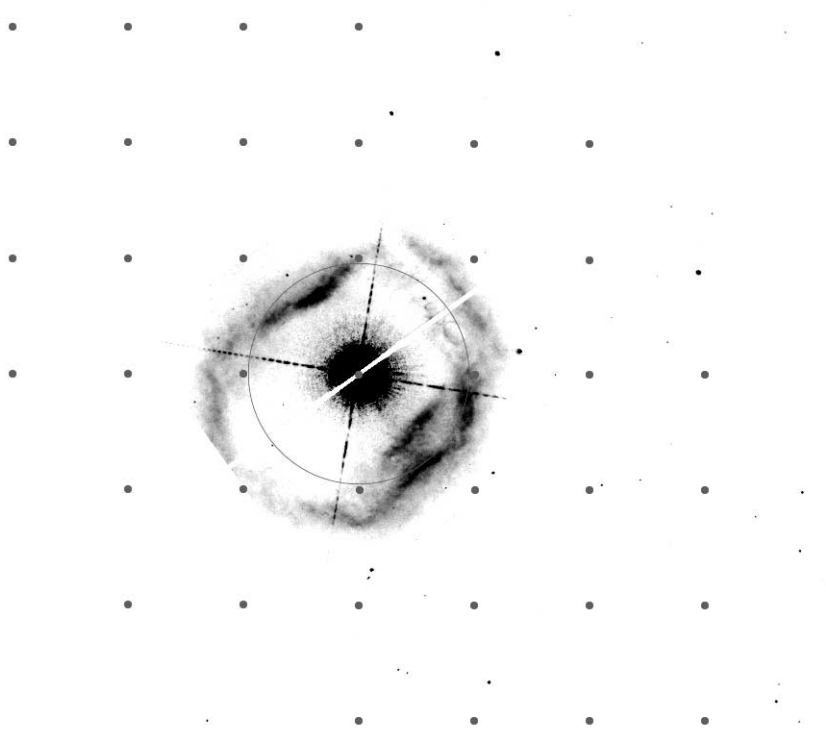

FIG. 2.—Hα image of the ejected nebula surrounding AG Car, on which are overlaid the pointings for the ^{12}CO $J = 2 \rightarrow 1$ map, which are spaced by 12″. The circle indicates the beamwidth for these observations (23″ diameter). North is up and east is to the left.

establish which components are intrinsic to AG Car and which are generated by the underlying interstellar region.

3.1. ^{12}CO $J = 1 \rightarrow 0$ *Map*

We investigated the circumstellar region around AG Car by making a map in right ascension of the ^{12}CO $J = 1 \rightarrow 0$ line, from 30′ west to 30′ east, and a smaller map in declination, from 0′ to 10′ to the north and to the south. The map is illustrated in Figure 4, where selected pointings in the north, east, south, and west regions are shown and compared with the observation on the star. The sampling of the observations is different in different regions: every 3′ in the east, every 2′ in the west, and selected pointings in the north-south direction (0′, −2′, −10′, +2′, +10′). Some of the pointings along the east-west direction show the two "narrow" components seen at the star's position, although at different levels of intensity, broadening, and separation. They are easily visible in the east region, although with remarkable variations in relative intensity (e.g., pointings at +12′ and +20′ in Fig. 4). They become very faint in the west region and almost disappear westward of 14′. They are visible in the south, but they are very weak in the north. In Figure 5, we have illustrated the motion of these two components in the east-west direction. Their velocity is reported, referenced to the local standard of rest, as a function of position with respect to the star (east to the left and west to the right). The overall motion is consistent with parallel sheets of neutral material at constant radial velocity and very different emissivity from point to point. From the line profiles in the maps, it is also clear that other narrow components are present, indicating that the source of this narrow CO component is in the complex motions of the underlying molecular gas and is *not* physically associated with AG Car.

The "broad" component appears to have a different origin. It is strongest in the pointing centered on the star and somewhat visible, although at lower intensity levels, in the spectra at +4′ and +2′. However, this "broad" component disappears completely beyond a few arcminutes from the central star, as can be seen in Figure 4. We have fitted a Gaussian of FWHM $\simeq$ 12 km s^{-1} to the "broad" component in each of the pointings in which it is visible, other than that on the central star, to estimate its intensity in the pointings adjacent to the star. We find that the "broad" component observed on the star is approximately a factor of 2 brighter than the average of the adjacent pointings in which the "broad" component is, at some level, visible (Fig. 6).

It is important to understand whether the emission is associated with the AG Car system. From the observations presented so far, it is clear that the emission is maximum in correspondence with AG Car and that it extends over a region that is possibly a few arcminutes in size. However, it is not possible, on the basis of these observations alone, to conclude whether the emission originates from the star and close circumstellar environment or from the surrounding nebula, which is rich in dust and most plausibly could also contain molecular gas. Unfortunately, the spatial resolution of the ^{12}CO $J = 1 \rightarrow 0$ observation is $\simeq$45″, which roughly corresponds to the spatial extent of the circumstellar nebula. The combination of the spatial resolution (45″) with the spatial sampling (2′) does not allow us to assess, from these observations alone, the origin of the detected emission.

We thus performed a second mapping, in the ^{12}CO $J = 2 \rightarrow 1$ line, with the expectation of being able to better

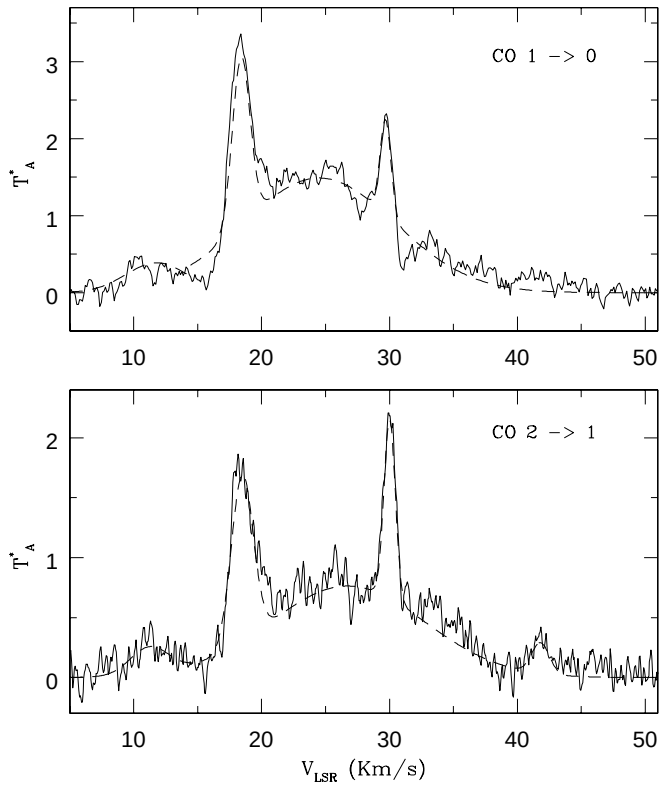

FIG. 3.—The ^{12}CO $J = 1 \rightarrow 0$ and $J = 2 \rightarrow 1$ profiles for the position centered on AG Car. A multiple-Gaussian fit has been performed for each observed line.

define the nature of this broad emission. In fact, in this observing mode the spatial resolution of SEST is almost a factor of 2 better (23″ beamwidth, compared with 45″).

3.2. ^{12}CO $J = 2 \rightarrow 1$ *Map*

The central section of the grid of ^{12}CO $J = 2 \rightarrow 1$ spectra covering the AG Car nebula is shown in Figure 7. The southwest quadrant of the nebula is of particular interest because it presents the highest concentration of gas and dust. This is the region where we would expect to detect the presence of molecular gas and, therefore, CO emission. Spectra of this region were taken in 1998 with a spacing of 12″ in both right ascension and declination. Additional maps of the remaining three quadrants were obtained a year later with the same observing configuration. The total spatial coverage of the ^{12}CO $J = 2 \rightarrow 1$ map is $\simeq$72″ in the two directions (east-west and north-south). The spectra cover the velocity range from -2 to 51 km s^{-1} and a range of beam temperature $T^*_{\rm mb}$ from -0.4 to 2.3 K. All spectra acquired at each position have been summed. As can be seen from the map, the ^{12}CO $J = 2 \rightarrow 1$ profiles are characterized by a complex structure of subpeaks in which a number of recurrent features can be identified. For example, the two dominant narrow components observed in the ^{12}CO $J = 1 \rightarrow 0$ spectra are detected in all the ^{12}CO $J = 2 \rightarrow 1$ profiles. Their morphology seems to change as function of position. In the south, the blueshifted component develops a broad and complex profile, with a number of subpeaks. The redshifted component increases in intensity with distance from the star, reaching a peak at Δdecl. $= -24''$. Additional, fainter, emission subpeaks are found between the two dominant components, and we note they tend to merge with the two dominant narrow components at increasing distance from the star.

Throughout the map, the same observational features are found, namely, (1) the two recurrent narrow emissions that eventually blend with secondary peaks, and (2) a broad component well visible in the pointing on the star and in many adjacent positions.

In order to better characterize the evolution of the emission components as a function of spatial position, we have applied a multiple-Gaussian fit to all the spectra in the ^{12}CO $J = 2 \rightarrow 1$ southwest map, to (1) identify the subpeaks detected at some of the offset positions and (2) track their motion as a function of position with respect to the star. The velocity-position map is shown in Figure 8, where we have identified 10 separate components in the ^{12}CO $J = 2 \rightarrow 1$ profile seen on the star (*top*) and tracked them at increasing distances from the star, in the southwest quadrant. Their velocities, reduced to the local standard of rest, are plotted as a function of distance from the star in the bottom panel of Figure 8. The filled and open circles indicate the two dominant narrow components—already discussed—at $V_{\rm lsr} = 18.5$ km s^{-1} and $V_{\rm lsr} = 29.7$ km s^{-1}, respectively. Five additional components are present in *all* positions observed; these are at $V_{\rm lsr} = 11$, 18.5, 21.5, 29.7, and 41 km s^{-1}. Other components are detected that have a more limited spatial extent: a feature at $V_{\rm lsr} = 13.5$ km s^{-1} appears only at distances farther than 17″ from the star, while a component at $V_{\rm lsr} = 26$ km s^{-1} disappears at distances farther than 38″. Two other components, at $V_{\rm lsr} = 27$ and $V_{\rm lsr} = 28$ km s^{-1}, develop at distances of 24″ and 27″, respectively. Finally, a component at $V_{\rm lsr} = 33.5$ km s^{-1} is not detected at distances greater than 12″. It is interesting to note that *all* detected components have constant velocity over the entire spatial range. This shows that the CO producing the narrow components is most likely in sheets of neutral material moving at constant velocity in the background or foreground of the AG Car system.

The most intriguing feature remains, however, the broad component observed in the spectra taken on and around the central star. It is still detected, but much less prominently, in the spectra on regions farther away from the star [e.g., (+12″, −24″) and (+12″, −12″)], most likely because of the fact that part of the beam (FWHM = 23″) still subtends the inner region. It seems unlikely that the emission originates in the AG Car optical nebula. In fact, the AG Car nebula is $\simeq$35″ in diameter. The brightest regions are located $\simeq$12″ from the star. If the CO emission were originating from the gaseous nebula, we would expect to detect little CO emission in the spectrum obtained on the star, and strong emission at distances 10″–20″ from the star. We observe exactly the opposite: the emission is stronger and best defined in the spectrum taken on the star and is much less prominent as soon as we depart from that position. This indicates clearly that the source of the broad CO component is in the close circumstellar environment of AG Car.

An independent confirmation of our conclusion comes from kinematic considerations: We have fitted a multiple-Gaussian function to the ^{12}CO $J = 2 \rightarrow 1$ profile acquired on the star [(0″, 0″)], to disentangle the broad component from the two narrow components that are detected at that position. The results of the fit are shown in Figure 3 (*bottom*). We have measured the broad component to have

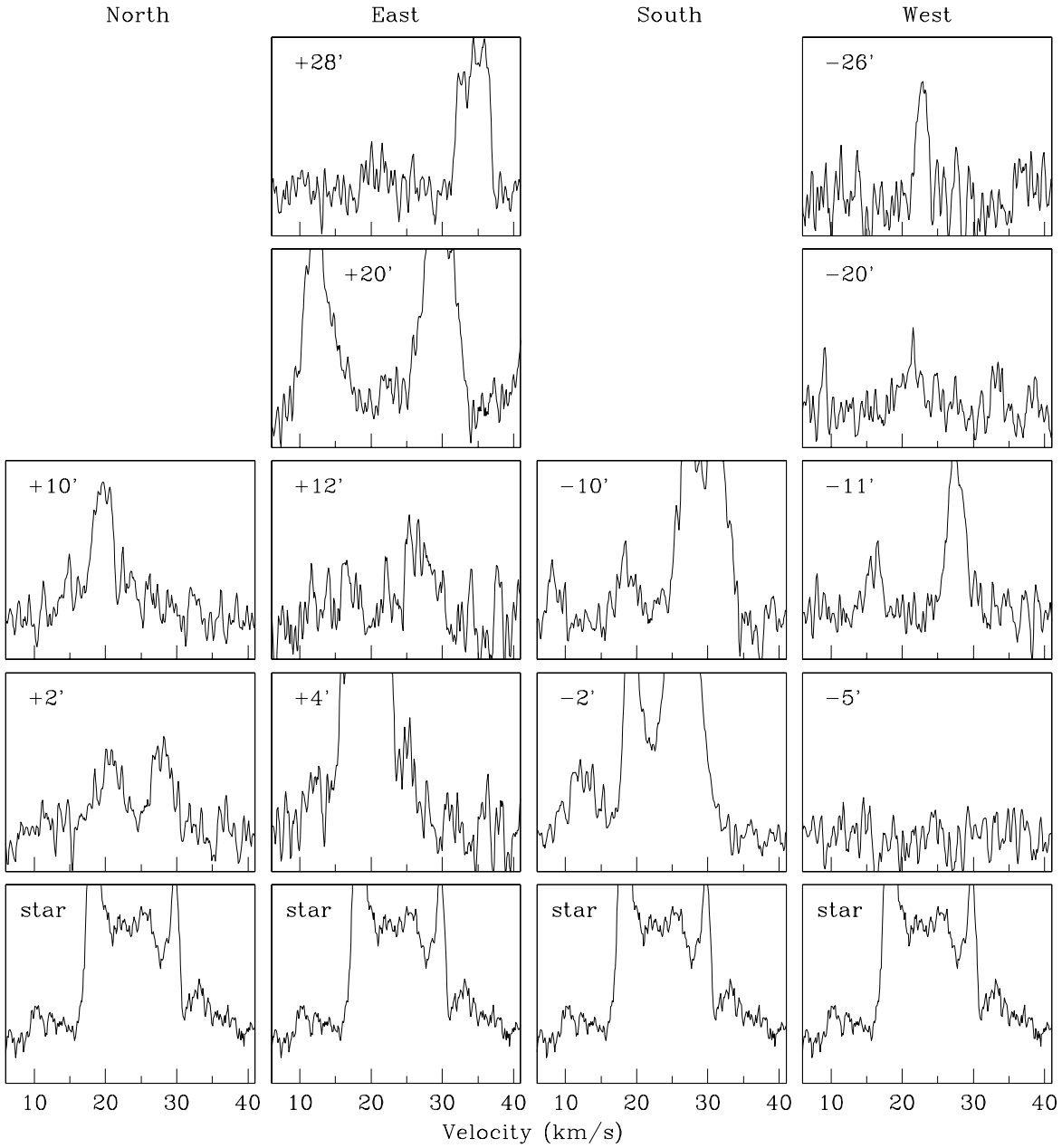

FIG. 4.—Map for the ^{12}CO $J = 1 \rightarrow 0$ observations of the region around AG Car. The numbers in the upper left of each panel provide the pointing location in arcminutes from the star (north, south, east, or west).

FWHM $\simeq$ 15 km s^{-1}, a peak velocity of 26.5 km s^{-1}, and a peak $T^*_{\rm mb}$ of 0.8 K. For comparison, in the top panel of Figure 3 we show the ^{12}CO $J = 1 \rightarrow 0$ line profile, which is very similar in morphology. In the case of the ^{12}CO $J = 1 \rightarrow 0$ line we have derived a peak $V_{\rm lsr}$ of 24.5 km s^{-1}, a peak T^*_A of 1.5 K, and a FWHM value of 14 km s^{-1}. This resulting expansion velocity of the outflow ($\simeq$7 km s^{-1}) is much lower than the expansion velocity of the optical nebula ($\simeq$70 km s^{-1}; Smith 1991). This difference in velocity again indicates that the CO emission does not originate at the location of the optical nebula, at a distance of $\simeq$20″ from the central star. The location and velocity of the broad CO component show that the CO emission comes from a region close to the star, with a small outflow velocity of $\simeq$7 km s^{-1}. Of course, this broad component could be due to a foreground or background cloud that happens to coincide with the position of the star. This is very unlikely, however, for the following reasons: first, because of the low probability of such a coincidence, and second, because of the larger width of the CO broad line compared with the other, narrower interstellar CO components.

4. DISCUSSION

Observations of the first-overtone band of CO at 2.3 μm in AG Car were attempted by McGregor et al. (1988). No CO emission was detected in the infrared spectrum of AG Car or in η Car or P Cygni, the three most well known Galactic LBVs. Our detection of broad emission in the submillimeter ^{12}CO $J = 2 \rightarrow 1$ and $J = 1 \rightarrow 0$ lines is,

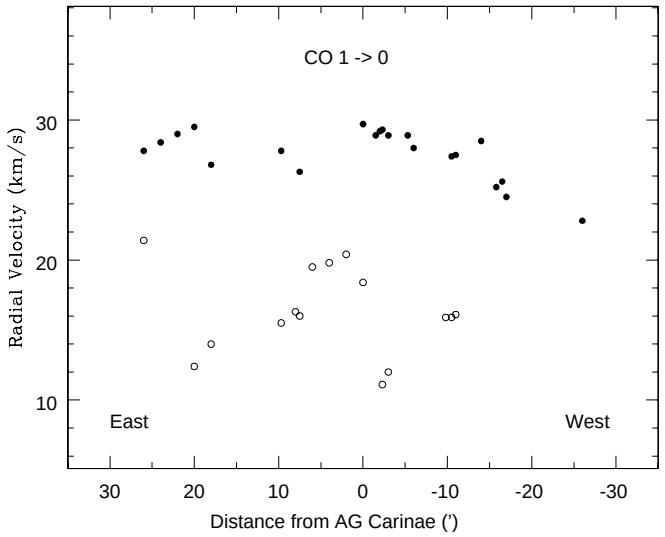

FIG. 5.—Radial velocity map of the two narrow components in the ^{12}CO $J = 1 \rightarrow 0$ emission as a function of position with respect to the star. The filled and empty circles identify the two components.

therefore, the first to date. This type of emission is typically found in carbon stars, which lose large amounts of matter in the form of a slow stellar wind and typically form circumstellar envelopes of gas and dust. The physical conditions of temperature and density in these envelopes are such that molecular species can form and survive and be shielded from the dissociating UV radiation field (Olofsson et al. 1988, 1993a, 1993b).

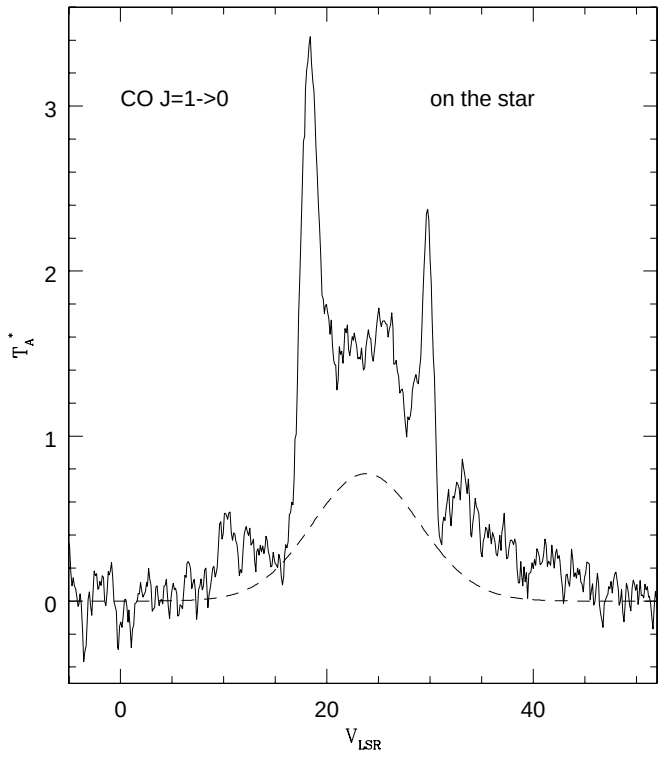

FIG. 6.—The mean interstellar, broad component (*dashed line*) superposed on the ^{12}CO $J = 1 \rightarrow 0$ profile observed on the star. The "on star" broad $J = 1 \rightarrow 0$ emission is a factor of 2 higher than its interstellar counterpart, and it is slightly broader.

Carbon stars come from low-mass progenitors and follow a very different evolutionary path compared with the much more massive counterparts discussed here. However, it is interesting to note that an inspection of the CO line profiles collected by Olofsson et al. (1993a, 1993b) from their large sample of Galactic bright carbon stars shows that the broad component observed in AG Car quite closely resembles similar features observed in the spectra of several stars in their sample. In general, the observed line profiles were found to lie in the middle of two extremes: the rectangular profile and the parabolic profile.

In determining the amount of CO, we have to make an assumption about its spatial and velocity distribution. The broad emission observed in AG Car closely mimics the standard parabolic profile (cf. Fig. 3). Such a profile can be due to an optically thin outflow if the beam size is smaller than the angular extension of the source. This option is excluded on the basis that we believe the emission to be unresolved. The parabolic profile can also be due to

1. An optically thick, spherically symmetric outflow at constant velocity; or
2. An optically thin wind with a nonspherical outflow or a velocity that is not constant with distance.

The presence of CO in close proximity to these very hot stars implies that the neutral material must be shielded from the stellar radiation. This is possible if the outflow is mainly in a disk (option 2). This disk could be either gravitationally bound, that is, a Keplerian disk, or an outflowing disk. As shown by Bjorkman (1998) and Kraus & Lamers (2002), effective shielding occurs in disks around B[e] stars, so that hydrogen remains neutral very close to the stars and CO can form at a distance of only a few stellar radii.

Moreover, the study of the chemical abundances in LBV nebulae (Lamers et al. 2001) and the currently accepted scenarios for the nebular ejection (Langer 1997) indicate that rotation must play an important role in the mixing and ejection of the nebula. Therefore, we cannot use the optically thick spherical approximation to estimate the amount of CO mass (option 1). Instead we will use the *optically thin* approximation to estimate a *lower limit* on the mass. The line luminosities of the 2.6 mm and the 1.3 mm lines are derived from the source monochromatic brightness $B_\nu(T)$ per steradian, where the brightness temperature $T (= T^*_{\rm mb})$ is the antenna temperature T^*_A corrected for the telescope efficiency. The net line flux is computed from the "on the star" broad component after subtraction of the mean interstellar contribution. The monochromatic brightness is actually the integral of the residual temperature profile as a function of frequency for the ^{12}CO $J = 1 \rightarrow 0$ line and the beam size of the telescope:

$$F_{2.6\,\rm mm} = \text{beam} \times \sum B_\nu(T)\Delta\nu \, . \qquad (1)$$

Therefore, the luminosity of the $J = 1 \rightarrow 0$ line turns out to be

$$L_{2.6\,\rm mm} = 4\pi D^2 F_{2.6\,\rm mm} = 1.3 \times 10^{-3}\ L_\odot \, . \qquad (2)$$

Similarly, we find for the 1.3 mm line

$$L_{1.3\,\rm mm} = 2.3 \times 10^{-3}\ L_\odot \, . \qquad (3)$$

If the emitting region is optically thin, the line luminosity can be expressed in terms of the total number of emitting CO molecules in the $J = 1$ level as $L_{2.6\,\rm mm} = N_{J=1} A_{1\rightarrow 0} h\nu$

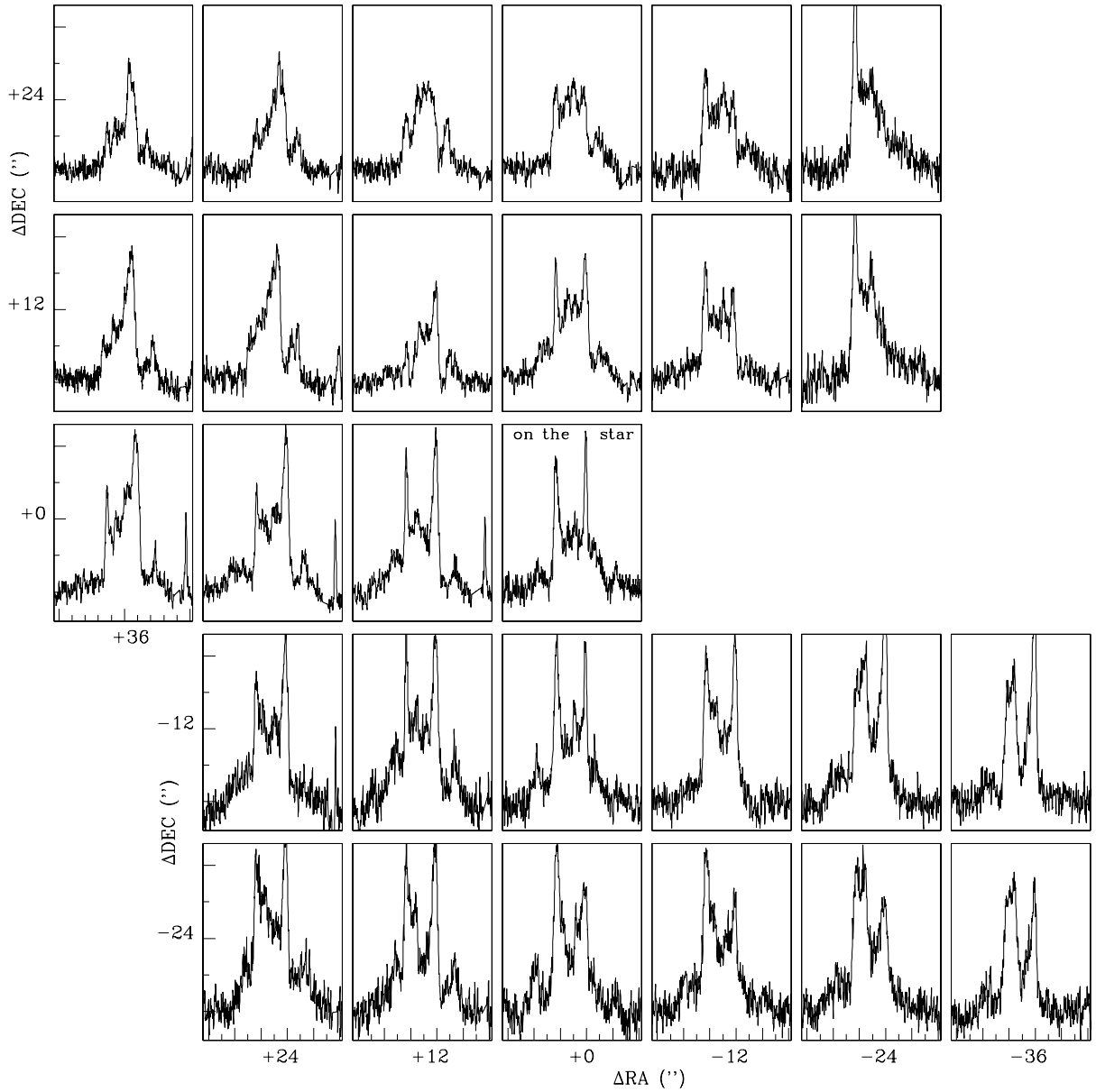

FIG. 7.—Map for the ^{12}CO $J = 2 \rightarrow 1$ observations of the region around AG Car. The numbers on the abscissa and ordinate axes provide the pointing location in arcseconds from the star (north, south, east, or west).

and similarly for the $J = 2 \rightarrow 1$ line, where the Einstein coefficients $A_{1\rightarrow0} = 6 \times 10^{-8}$ s^{-1} and $A_{2\rightarrow1} = 7 \times 10^{-7}$ s^{-1}. The population of the $J = 1$ level can be expressed in terms of an excitation temperature as

$$N_{J=1} = N_{J=0} \frac{g_u}{g_l} \exp\left(-\chi/kT_{\rm exc}\right) \quad (4)$$

with $g_u = 3$ and $g_l = 1$ and $\chi = 4.77 \times 10^{-4}$ eV. The excitation temperature is at least as high as that of the 2.7 K background radiation. This implies that $N_{J=0} < 2.6 N_{J=1}$ and $N_{\rm tot} < 3.6 N_{J=1}$. We can estimate the excitation temperature from a comparison of the line luminosities of the ^{12}CO $J = 2 \rightarrow 1$ and $J = 1 \rightarrow 0$ lines, which is $L_{2\rightarrow1}/L_{1\rightarrow0} = 1.7$. With the parameters given above, we find that $N_{J=2}/N_{J=1} = 0.090$, which corresponds to an excitation temperature between these two levels of 3.8 K. Note that this is the excitation temperature produced by collisions with H_2 molecules and not the gas temperature, which can be much higher. Adopting this value for both excitation steps, we find that $N_{\rm tot} = N_{J=0} + N_{J=1} + N_{J=2} = 2.52 N_{J=1}$. We will adopt this ratio for the derivation of the lower limit to the CO mass.

From the values of $L_{2.6\,\rm mm}$ and $L_{1.3\,\rm mm}$, we find that the total number of CO molecules required to produce these line strengths is 2.3×10^{53}. This implies a minimum CO mass of $(5.2\text{–}5.4) \times 10^{-3}\, M_\odot$.

We can estimate the total amount of molecular gas by quantifying the present fraction of CO. Studies of the CNO abundances in the nebulae of LBVs by Smith et al. (1998) and Lamers et al. (2001) show that the nebula of AG Car consists roughly of 80% processed material in which carbon is severely depleted and 20% of unprocessed material. This

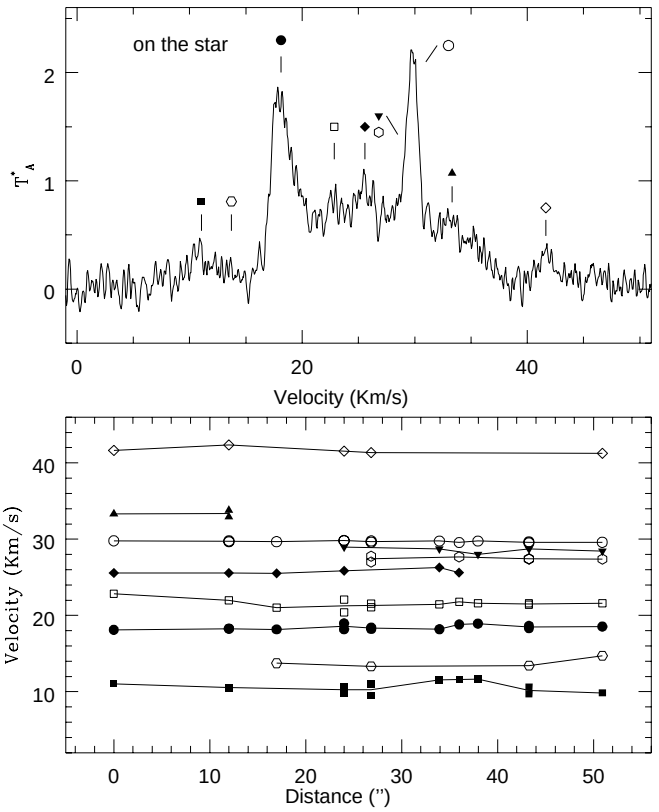

FIG. 8.—Multiple-Gaussian fit to the various components present in the ^{12}CO $J = 2 \rightarrow 1$ profile on the star (*top*). The various components are identified and tracked to a distance of 50″ from the star (*bottom*). They move in parallel sheets, and they show a limited spatial extent. Most likely, they belong to the underlying molecular gas region.

suggests that the mass fraction of carbon is depleted by about a factor of 5 relative to the initial composition, for which the mass fraction of carbon is 4.9×10^{-3} in Population I gas. Oxygen is also depleted, but the C/O ratio will still be smaller than unity, so that the CO abundance is set by the carbon abundance. If all the carbon is locked in CO, which is a reasonable assumption for a shielded region, the mass fraction of $^{12}C/^{16}O$ is 28/12 times the mass fraction of C. On the assumption that the CO emission was generated when AG Car was an evolved object, the CO mass fraction would then be $(1/5)(28/12)(4.9 \times 10^{-3}) = 2.3 \times 10^{-3}$. Accounting for this fraction, we find a total mass for the molecular region of 2.8 $M_\odot$. With this estimated minimum mass, and a maximum radius for the unresolved CO emitting region of about 30″ in diameter, we find that the optical depths of the CO lines are $\tau_{1\rightarrow0} \simeq 8$ and $\tau_{2\rightarrow1} \simeq 4$. So the lines are marginally optically thick and the mass estimate is indeed a lower limit. The H_2 density, derived from the CO column density and the ratio $n(H_2)/n(CO) \simeq 6 \times 10^3$, is at least 5×10^2 molecules cm^{-3}.

This cool gas is most likely concentrated in the outer regions of a circumstellar disk. Such a disk might be the result of a strong equatorial mass loss, possibly combined with wind compression, similar to the disks of B[e] supergiants (Zickgraf et al. 1986; Bjorkman 1998; Cassinelli 1998), or due to an outburst when the star reached its Ω-limit, which is the rotationally modified Eddington limit (Langer 1997). In the case of AG Car, some circumstantial evidence already exists that the star might host a gaseous disk (which is required to shield the CO in its outer layers from the stellar radiation), based on several independent observational factors:

1. *Bipolarity of the circumstellar nebula*.—Especially in the light of the continuum, the ejected nebula surrounding AG Car displays a remarkable axisymmetry (Nota et al. 1996), which could have been produced by a strong stellar wind interacting with a preexisting equatorial enhancement.
2. *Variability in the intrinsic polarization* (≃1.2%).—Very large variations in AG Car's linear polarization with time have been observed at UV and optical wavelengths (Schulte-Ladbeck et al. 1994; Leitherer et al. 1994). The polarization is found to vary along a preferred position angle that is co-aligned with the major axis of the circumstellar nebula. Schulte-Ladbeck et al. (1994) and Leitherer et al. (1994) interpret this finding as the presence of a strong anisotropy in the stellar wind.
3. *Coexistence of different wind components in the UV line profiles*.—The UV spectra show both the presence of recombination lines due to a slow, dense wind and UV P Cygni profiles indicative of a faster, less dense wind (Leitherer et al. 1994). This two-component wind structure is very reminiscent of the wind conditions in B[e] stars, where the slow, dense wind is usually referred to as a circumstellar disk (Zickgraf et al. 1986; Kraus & Krügel 2002).

The comparison with the B[e] supergiants is also interesting. B[e] stars share approximately the same location in the H-R diagram with LBVs, although at slightly cooler temperatures. B[e] supergiants show clear evidence of a fast, low-density wind with $V \simeq 1000$ km s^{-1}, which can be seen in the UV resonance lines, and a more slowly expanding equatorial disk with $V \simeq 100$–200 km s^{-1} that can be seen in the Balmer lines, in the low-excitation permitted emission lines of the metals, and in the forbidden emission lines of [Fe II] and [O I].

Zickgraf et al. (1986) have explained the observed bimodality in terms of a two-component wind, developing along the polar axis and on the equatorial plane of the stars. Such a structure can be explained by the model of rotation-induced bistability (Lamers & Pauldrach 1991; Pelupessy, Lamers, & Vink 2000). The polar wind is radiation driven, hot but not dense, expanding at higher speed. It is responsible for the strong P Cygni emissions of the UV resonance lines. The equatorial outflow, which is also radiation driven, but by ions of lower ionization stages than the polar wind, is cooler and denser, moving at lower velocity. The conditions in the dense equatorial outflow allow shielding of the heavy elements and are met by an equatorial enhancement of the stellar wind, which is also referred to as a disk. This disk is possibly further compressed via the wind-compressed disk mechanism (Bjorkman & Cassinelli 1993; Lamers & Cassinelli 1999). The circumstellar disk prevents dust from being destroyed by the stellar radiation and may well explain the characteristic strong infrared excess observed in B[e] supergiants due to thermal emission from dust at $T \simeq 1000$ K (Bjorkman 1998).

AG Car is not the only LBV for which the possible presence of a disk has been indicated by a number of independent observations. HR Carinae, for example, which is to date the most plausible LBV candidate for having a disk, shares some of the same observational evidence: (1) a bipolar nebula; (2) CO overtone emission detected in the infrared spectrum (McGregor et al. 1988), indicative of a cool (a

few thousand kelvins) and dense ($\simeq 10^{10}$ cm^{-3}) region of circumstellar gas; and (3) evidence for the presence of intrinsic polarization, from the change of polarization at the Hα emission line with respect to the continuum (Clampin et al. 1995). These results imply that the scattering material in close proximity to the star is also not distributed with spherical symmetry. In addition, in similarity to AG Car, the intrinsic polarization vector turns out to be coarsely perpendicular to the nebular major axis.

It is interesting to understand why McGregor et al. (1988) failed to detect any near-IR CO overtone emission in AG Car, while detecting it in HR Car. McGregor et al. observed HR Car four times between 1984 and 1986. In 1984 March and June, they detected the three CO overtone bands at 2.295, 2.324, and 2.354 μm. In 1985 March and 1986 February, they reobserved the star but could only obtain an upper limit to the flux. Morris et al. (1997) reobserved HR Car in 1995 November with *ISO* and again detected the presence of the three CO band heads. They found that a combination of a bistable wind with rapid rotation or wind compression forming a disk would supply the density and shielding required to explain the observed CO flux. In addition, they found that the variability of the CO overtone emission was in phase with the variations in the V magnitude, that is, the CO overtone would be detected when the light curve was at a minimum. Morris et al. (1997) explained this observed variability with optical depth variations as predicted by the theory of bistable line-driven winds (Pauldrach & Puls 1990) and for bistable disks by Lamers & Pauldrach (1991).

The nondetection of CO band heads in AG Car could also be explained by a similar mechanism. AG Car was observed three times: in 1984 March, 1984 June, and 1985 January, always with upper limits obtained to the flux determination of the three CO bands. When comparing with the optical light curve provided by Leitherer et al. (1994, their Fig. 1), we find that AG Car was shifting from maximum to minimum in 1982–1985, reaching a stable minimum at the beginning of 1985. It is unfortunate that no subsequent CO observations were taken.

5. CONCLUSIONS

We have presented the first detection of ^{12}CO $J = 2 \rightarrow 1$ and $J = 1 \rightarrow 0$ emission from the luminous blue variable AG Carinae. The emission is spatially unresolved. We believe it to be spatially localized, rather than extended, and most likely associated with the immediate circumstellar region of AG Car, that is, inside the optical nebula. Both detected CO lines are characterized by a pseudo-Gaussian profile of FWHM $\simeq$ 15 km s^{-1}, indicating a slowly expanding region of molecular gas in close proximity to the hot central star. We have explored two possible scenarios to explain the observed profile: a circumstellar envelope, similar to carbon stars, and a circumstellar disk. We believe that the option of the circumstellar disk is preferable to provide the shielding necessary for the CO molecules to survive.

What is the origin of the CO emission? The outflow velocity ($\simeq$7 km s^{-1}) is atypically low when compared with the wind velocities of LBVs ($V_{\rm inf} > 100$–200 km s^{-1}). As already mentioned, the CO velocity is also much slower than the expansion velocity of the optical nebula ($\simeq$70 km s^{-1}), with which it is unlikely associated. In terms of absolute values, slow winds are usually found in red supergiants. The question whether AG Car spent any time as an RSG is still open and argued on the basis of independent observational facts.

Smith et al. (1988) and Waters et al. (1998) argued that the abundances of the nebula and the composition of the dust would be in agreement with the ejection of the nebula as an RSG. Alternatively, Lamers et al. (2001) have shown that the abundances, the velocity, the dynamical age, and the morphology of the nebula are all consistent with its being ejected immediately after the main-sequence phase of a rapidly rotating star. In that case, the star cannot have been an RSG in the evolutionary sense (i.e., a massive star with a very extended convective envelope), but it may have resembled an RSG during an outburst phase, when the wind was optically thick, the effective radius very large, and the outflow velocity very low.

We consider several possible origins for the CO emission:

1. In the scenario proposed by Smith et al. (1998), which includes an RSG phase, or by Lamers et al. (2001), which includes a brief RSG-like phase, the molecular outflow could have originated during the RSG phase and survived protected by the disk that likely formed when the star, evolving as an LBV to the blue side of the H-R diagram, developed its fast wind. This could easily explain the low expansion velocity.

2. Alternatively, the CO may originate at the outer regions of a circumstellar disk, similar to the case of the B[e] stars. In this case, the low velocity is difficult to explain. In normal B[e] stars the outflow velocity is on the order of 100 km s^{-1}, even at large distances, as shown by the forbidden lines (Zickgraf et al. 1986). This is much larger than the value of 7 km s^{-1} that we observe.

3. Or, the CO emission may originate at the interaction zone at the edge of the interstellar bubble that was blown by the star. The maximum size of the emitting region ($<1'$) corresponds to a radius of about 1 pc. The amount of mass lost by the star in its main-sequence phase is about 10 $M_\odot$. The observed amount of molecular gas is $\simeq$3 $M_\odot$, which is only about one-fourth the total mass of the shocked gas at the edge of the bubble. The main problem with this interpretation is the small radius of the unresolved CO emitting region (diameter less than 30$''$, or 0.9 pc) compared with the predicted much larger size (several tens of parsecs) of a bubble blown by a spherical wind from a massive star with a velocity of 1000 km s^{-1} over 4×10^6 yr (see, e.g., Lamers & Cassinelli 1999, p. 369). However, if the wind were aspherical—for example, concentrated in a disk as a result of the rapid rotation—the expansion speed of the interaction region in the equatorial plane would be much smaller because the bubble could more easily expand in the other direction. This might result in a high-density and very low velocity "waist" to the bipolar interstellar bubble, from which the observed CO emission might originate.

We estimate a lower limit to the mass of the molecular region of 2.8 $M_\odot$. This is smaller than, but still comparable to, the mass of ionized gas present in the circumstellar environment (4.2 $M_\odot$). The implication is that the molecular gas fraction can contribute significantly to the overall mass lost from the central star in its post–main-sequence evolution, and therefore one should be careful when assuming that the ionized gas mass well approximates, at least in the case of AG Carinae, the total mass lost.

A. P. M. would like to acknowledge financial support from NASA Astrophysics Data Program grants NAG 5-2999 and NAG 5-6854 and a grant from NASA administered by the AAS. A. P. M. and H. J. G. L. M. L. would also like to thank the STScI Collaborative Visitor Program for the funding and the hospitality.

REFERENCES

Bjorkman, J. E. 1998, in B[e] Stars, ed. A.-M. Hubert & C. Jaschek (Dordrecht: Kluwer), 189
Bjorkman, J. E., & Cassinelli, J. P. 1993, ApJ, 409, 429
Cassinelli, J. P. 1998, in B[e] Stars, ed. A.-M. Hubert & C. Jaschek (Dordrecht: Kluwer), 177
Clampin, M., Schulte-Ladbeck, R. E., Nota, A., Robberto, M., Paresce, F., & Clayton, G. C. 1995, AJ, 110, 251
Heske, A. 1990, A&A, 229, 494
Humphreys, R., & Davidson, K. 1979, ApJ, 232, 409
Humphreys, R. M., Lamers, H. J. G. L. M., Hoekzema, A., & Cassatella, A. 1989, A&A, 218, L17
Knapp, G. R. & Morris, M. 1985, ApJ, 292, 640 (erratum 303, 521 [1986])
Kraus, M., & Krügel, E. 2002, A&A, in press
Kraus, M., & Lamers, H. J. G. L. M. 2002, in preparation
Lamers, H. J. G. L. M. 1986, in IAU Symp. 116, Luminous Stars and Associations in Galaxies, ed. C. W. H. de Loore, A. J. Willis, & P. Laskarides (Dordrecht: Reidel), 157
Lamers, H. J. G. L. M., & Cassinelli, J. P. 1999, Introduction to Stellar Winds (Cambridge: Cambridge Univ. Press), chap. 11
Lamers, H. J. G. L. M., Nota, A., Panagia, N., Smith, L. J., & Langer, N. 2001, ApJ, 551, 764
Lamers, H. J. G. L. M., & Pauldrach, A. W. A. 1991, A&A, 244, L5
Langer, N. 1997, in ASP Conf. Ser. 120, Luminous Blue Variables, ed. A. Nota & H. J. G. L. M. Lamers (San Francisco: ASP), 83
Langer, N., Hamann, W.-R., Lennon, M., Najarro, F., Pauldrach, A. W. A., & Puls, J. 1994, A&A, 290, 819
Leitherer, C., et al. 1994, ApJ, 428, 292
McGregor, P. J., Hillier, D. J., & Hyland, A. R. 1988, ApJ, 334, 639
Morris, P. W., Voors, R. H. M., Lamers, H. J. G. L. M., & Eenens, P. R. J. 1997, in ASP Conf. Ser. 120, Luminous Blue Variables, ed. A. Nota & H. J. G. L. M. Lamers (San Francisco: ASP), 20
Morris, P. W., et al. 1999, Nature, 402, 502
Nota, A., Clampin, M., García-Segura, G., Leitherer, C., & Langer, N. 1996, in Science with the *Hubble Space Telescope*: II, ed. P. Benvenuti, F. D. Macchetto, & E. J. Schreier (Baltimore: STScI), 398
Nota, A., Leitherer, C., Clampin, M., Greenfield, P., & Golimowski, D. A. 1992, ApJ, 398, 621
Nota, A., Livio, M., Clampin, M., & Schulte-Ladbeck, R. 1995, ApJ, 448, 788
Olofsson, H., Eriksson, K., & Gustafsson, B. 1988, A&A, 196, L1
Olofsson, H., Eriksson, K., Gustafsson, B., & Carlström, U. 1993a, ApJS, 87, 267
———. 1993b, ApJS, 87, 305
Paresce, F., & Nota, A. 1989, ApJ, 341, L83
Pasquali, A., Langer, N., Schmutz, W., Leitherer, C., Nota, A., Hubeny, I., & Moffat, A. F. J. 1997, ApJ, 478, 340
Pauldrach, A. W. A., & Puls, J. 1990, A&A, 237, 409
Pelupessy, I., Lamers, H. J. G. L. M., & Vink, J. S. 2000, A&A, 359, 695
Schulte-Ladbeck, R. E., Clayton, G. C., Hillier, D. J., Harries, T. J., & Howarth, I. D. 1994, ApJ, 429, 846
Smith, L. J. 1991, in IAU Symp. 143, Wolf-Rayet Stars and Interrelations with Other Massive Stars in Galaxies, ed. K. A. van der Hucht & B. Hidayat (Dordrecht: Kluwer), 385
Smith, L. J., Nota, A., Pasquali, A., Leitherer, C., Clampin, M., & Crowther, P. A. 1998, ApJ, 503, 278
Thackeray, A. D. 1950, MNRAS, 110, 524
Voors, R. H. M., et al. 2000, A&A, 356, 501
Voors, R. H. M., Waters, L. B. F. M., Trams, N. R., & Käufl, H. U. 1997, A&A, 321, L21
Waters, L. B. F. M., Morris, P. W., Voors, R. H. M., Lamers, H. J. G. L. M., & Trams, N. R. 1998, Ap&SS, 255, 179
Waters, L. B. F. M., Voors, R. H. M., Morris, P. W., Trams, N. R., de Koter, A., & Lamers, H. J. G. L. M. 1999, in IAU Colloq. 169, Variable and Non-spherical Stellar Winds in Luminous Hot Stars, ed. B. Wolf, O. Stahl, & A. W. Fullerton (Lecture Notes in Physics, 523) (Berlin: Springer), 381
Zickgraf, F.-J., Wolf, B., Stahl. O., Leitherer, C., & Appenzeller, I. 1986, A&A, 163, 119